

Macromolecules

Volume 28, Number 23

November 6, 1995

© Copyright 1995 by the American Chemical Society

A Small-Angle X-ray Scattering Study of High-Density Polyethylene and Ultrahigh Molecular Weight Polyethylene

A. Bellare*

*Department of Orthopedic Surgery, Brigham and Women's Hospital,
Boston, Massachusetts 02115*

H. Schnablegger[†] and R. E. Cohen

*Department of Chemical Engineering, Massachusetts Institute of Technology,
Cambridge, Massachusetts 02139*

*Received March 3, 1995; Revised Manuscript Received July 10, 1995**

ABSTRACT: Small-angle X-ray scattering was used to compare the morphology of extruded ultrahigh molecular weight polyethylene (UHMWPE) and melt-crystallized high-density polyethylene (HDPE). The crystalline morphology of UHMWPE has a low degree of order, rendering direct methods of analysis of the scattering curves unsuitable. We have demonstrated that the indirect transformation method, requiring no extrapolation of the scattering curve, can be used to obtain the one-dimensional correlation functions for these dense lamellar systems. The lamellar morphology of UHMWPE contained a large distribution of lamellar thicknesses, diffuse interfaces, and a large variation of interlamellar spacing as compared to those features in HDPE. The interlamellar spacing of extruded UHMWPE determined from the one-dimensional correlation function was 50 nm and that of melt-crystallized HDPE was 26 nm. The amorphous zone thickness of HDPE was 8 nm.

Introduction

The morphology of heterogeneous polymers can be characterized by a variety of experimental methods depending on the length scale at which the morphology is to be observed. In this article we shall confine our morphological analyses to the nanometer scale. Transmission electron microscopy (TEM) is the technique most commonly used to characterize the morphology at this size scale. However, availability of high-flux X-ray and neutron sources and advances in scattering methods have increased the usage of small-angle scattering for the characterization of polymer morphology. Scattering methods provide more accurate quantitative information of the morphology that may be distorted in TEM due to sample preparation techniques such as ultramicrotoming and staining. Furthermore, scattering methods provide information on the morphology that is averaged in three dimensions whereas TEM micrographs, although often striking in their visual impact, are two-dimensional projections of the local morphology. In general, the two techniques are complementary.

Characterization of the scattering medium using SAXS can be performed by a number of methods. Tsvankin fitted the experimental scattering curve $I(q)$ with curves generated by model electron density profiles, $\rho(r)$.¹ Vonk and Kortleve developed a method to obtain the experimental one-dimensional correlation function, $\gamma(r)$ by inverse Fourier transformation of the experimental scattering function, $I(q)$.² This method simplifies the interpretation of morphology since $\gamma(r)$ has real space coordinates and is proportional to the autoconvolution of the electron density distribution, $\rho(r)$. Vonk and Kortleve developed procedures to fit the experimentally determined $\gamma(r)$ with a $\gamma(r)$ function calculated from proposed electron-density profiles. However, this method requires uncertain extrapolation of the experimental scattering intensities to scattering angles of 0 and ∞ ; the extrapolation is required because any discontinuity in $I(q)$ results in superposition of oscillations in the corresponding correlation function. Strobl used integral scattering intensities of long-period scattering peaks to characterize lamellar structures for samples with a highly ordered morphology.³ For LDPE samples with a low degree of order, Strobl et al. obtained the experimental $\gamma(r)$ from $I(q)$ extrapolated to q values of 0 and ∞ .^{4,5} The experimental $\gamma(r)$ was used to obtain

* Present address: Max Planck Institute for Colloids, Kantstrasse 55, D-14513 Teltow-Seehof, Germany.

[†] Abstract published in *Advance ACS Abstracts*, October 1, 1995.

the crystallinity and specific interfacial area of crystallites. Absolute intensity measurements enabled the determination of electron density differences between amorphous and crystalline domains.

In the present work we have used a method developed by Glatter^{6,7} to determine the lamellar morphology of melt-crystallized high-density polyethylene (HDPE) and extruded rod stock of ultrahigh molecular weight polyethylene (UHMWPE). We analyze their morphologies by comparison of their pair distance distribution function (PDDF), $p(r)$, obtained by an indirect Fourier transformation of the scattering function $I(q)$.^{6,7} The method requires no extrapolation of the scattering function. It is possible to obtain information on important features of the lamellar structure without laborious measurements of absolute intensities.

Experimental Procedure

The two types of polyethylene used in this study were HDPE and UHMWPE. The HDPE was Petrothene, LS606-00 supplied by Quantum (USI Division, Cincinnati, OH). The molecular weight was 55 000 with a polydispersity, M_w/M_n , of 4.8, and the melt flow index was 9–11 g/10 min (ASTM D-1238). Pellets of HDPE were compression molded into sheets of 1 mm thickness. The pellets were maintained between the hot platens of a Carver hydraulic press at 175 °C for 10 min and quenched in cold water.

The UHMWPE was in the form of rod stock (Westlake Plastics) obtained by ram extrusion of GUR 415 powder (Hoechst-Celanese). The molecular weight of GUR 415 is 6×10^6 , determined from intrinsic viscosity measurements (ASTM D-4020); the melt flow index for UHMWPE is essentially zero. The value of the molecular weight is expected to be higher than the reported value since the intrinsic viscosity method is known to underestimate the molecular weight of UHMWPE.⁹ A sheet of UHMWPE of 1 mm thickness was machined from a section of extruded rod stock. Two-dimensional SAXS intensities were collected along orthogonal directions for each sample to ascertain that the samples were isotropic. This sample isotropy was confirmed by wide-angle X-ray pole figure analyses.

A Rigaku rotating-anode Cu K α X-ray source operating at 40 kV and 30 mA was used to perform the SAXS measurements. Data were obtained in the form of scattered X-ray intensities I (arbitrary units of counts per second) as a function of the scattering vector $q = (4\pi/\lambda) \sin \theta$ (units of nm⁻¹), where θ is half the scattering angle and λ is the wavelength of radiation (=0.154 nm for Cu K α). The X-ray beam from the point source was collimated using double-focusing Charles Supper mirrors. The beam profile was measured and used directly to desmear the scattering function. The beam diameter obtained from the full width at half-maximum (fwhm) of the beam profile corresponded to a q value of 0.006 nm⁻¹. The scattered X-rays passed through a helium-filled tube to reduce background scattering and to increase the signal/noise ratio. A two-dimensional Siemens detector placed at a distance of 280 cm from the sample was used to detect the scattered X-rays between $q_{\min} = 0.06$ up to $q_{\max} = 0.7$ nm⁻¹. The detector was equipped with a position decoding circuit and controlled by a dedicated Nicolet computer. Data analysis was performed in a DOS-based personal computer using ITP and DECON computer programs developed by Glatter.^{6–8}

Results and Discussion

The experimental scattering functions $I(q)$ were obtained for melt-crystallized sheets of HDPE and UHMWPE and are presented in Figure 1. There is a low degree of order in both morphologies, evident from the absence of resolvable higher order peaks. The low order in HDPE is attributed to crystallization induced by quenching, while the order in UHMWPE is usually low due to its high molecular weight. Both compression-

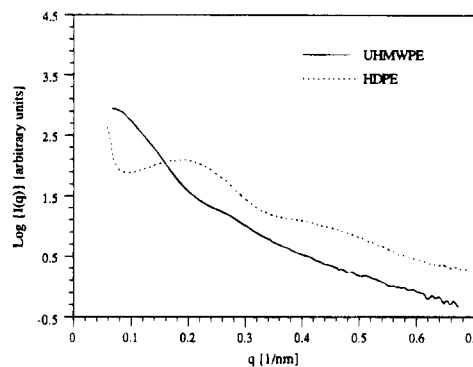


Figure 1. Semilogarithmic plot of the experimental scattering intensity, $\log \{I(q)\}$, versus the scattering vector q for melt-crystallized HDPE (dotted curve) and extruded UHMWPE (solid curve).

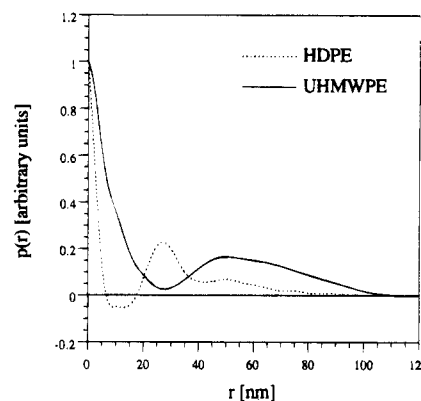


Figure 2. Plot of the experimental pair distance distribution function, $p(r)$, versus radial distance r for HDPE (dotted curve) and UHMWPE (solid curve). The $p(r)$ values are normalized to be equal to 1 at the origin.

molded sheets and ram-extruded rods of UHMWPE have shown morphology of a low degree of order. In the case of UHMWPE, the absence of even a first-order peak shows a lower degree of order than that of the HDPE sample. This makes it impossible to obtain even the long period directly from the scattering curve. It is evident from Figure 1 that the morphology of UHMWPE and HDPE cannot be compared effectively by analysis of their SAXS scattering curves.

The pair distance distribution function can be obtained by Fourier transformation of the scattering function:

$$p(r) = \frac{1}{2\pi^2 A} \int_0^\infty q^2 I(q) \cos(qr) dq \quad (1)$$

where $p(r)$ is the pair distance distribution function, PDDF, along a direction perpendicular to the lamellar surface, r is a real space distance (units of nm), q is the scattering vector, A is the area of the lamella, and $I(q)$ is the experimental scattering function. However, a direct transformation requires knowledge of the scattering function $I(q)$ over the entire range of scattering vectors, i.e., q values between 0 and ∞ .^{2,4,5} We used the computer program ITP developed by Glatter^{6,7} to perform an indirect Fourier transformation in which the transformation occurs between q_{\min} , the lowest experimentally acceptable scattering angle, and q_{\max} , the maximum value at which the experimental scattering intensities were measured. No data points outside the acceptable range of detection were considered, and the indirect Fourier transformation does not require data points in the corresponding regions to be set to zero.

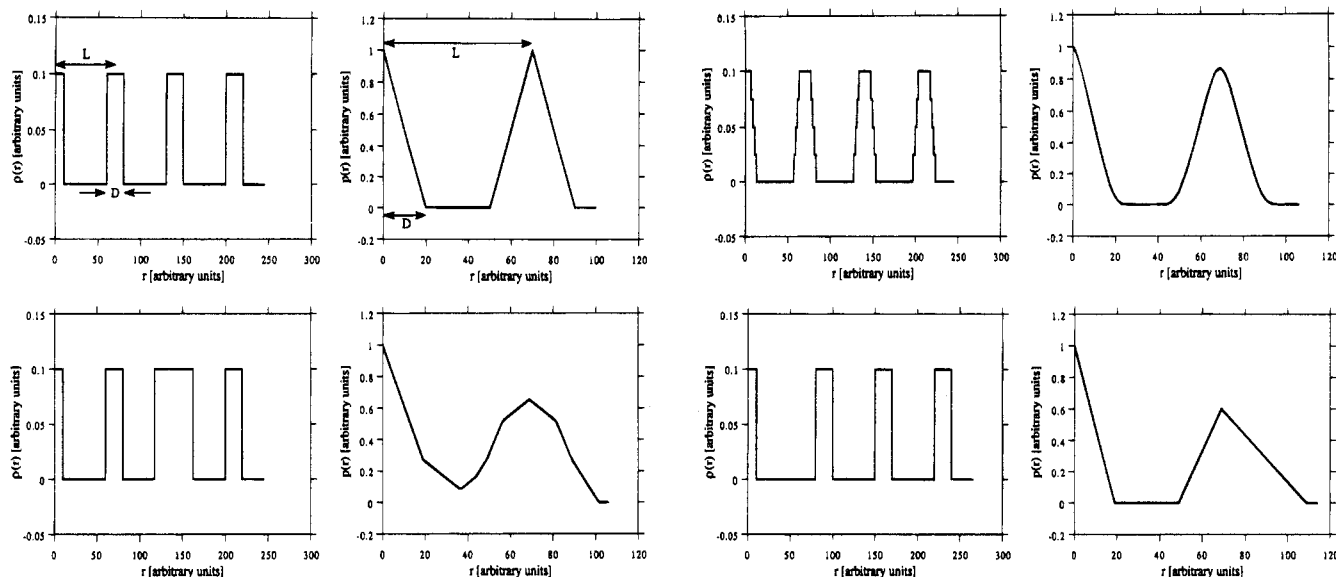


Figure 3. Plots of electron density distribution, $\rho(r)$, versus r (left) and the corresponding PDDF, $p(r)$, versus r (right). Panel a is a schematic of $\rho(r)$ versus r and the corresponding $p(r)$ versus r for a constant domain thickness, D , constant interdomain spacing, L , and sharp interface. Panels b–d are plots of $\rho(r)$ versus r and their corresponding $p(r)$ versus r obtained using program DECON, demonstrating the effect of (b) diffuse interface, (c) variation in thickness at constant interdomain spacing, and (d) variation in interdomain spacing at constant domain thickness.

Termination effects caused by truncation of the data at q_{\min} and q_{\max} were minimized using the program ITP.

The PDDF of HDPE and UHMWPE are presented in Figure 2. The differences between the morphologies of these samples is far more evident from a comparison of their PDDFs than from their scattering functions. The noteworthy features of these PDDFs that capture the differences between their respective lamellar morphologies are as follows:

(1) The $p(r)$ of UHMWPE has a distinct initial concave-downward curvature at the origin, unlike the $p(r)$ of HDPE.

(2) The initial descending region of $p(r)$ for HDPE is essentially linear and that of UHMWPE shows a variable slope, the magnitude of which initially increases and then decreases.

(3) There is a plateau region in $p(r)$ of HDPE following the initial linear region. No such plateau exists in the $p(r)$ of UHMWPE.

(4) The first-neighbor peak of HDPE is symmetric, unlike that of UHMWPE, which is asymmetric.

(5) The first-neighbor peak, which represents the interlamellar spacing (long period, L), appears at 26 nm for HDPE and at 50 nm for UHMWPE. A second-order peak is observed only for HDPE, suggesting its higher degree of order.

The interpretation of the first four observations in terms of features of the lamellar structures of HDPE and UHMWPE is assisted by generating one-dimensional correlation functions $\gamma(r)$ functions from model $\rho(r)$ profiles. One can directly compare $p(r)$ with $\gamma(r)$ for lamellar morphologies since they are identical to each other.⁸ Therefore in the case of lamellar morphology, $p(r)$ can be obtained from $\rho(r)$ by autoconvolution:

$$p(r) = \int_{-\infty}^{\infty} \rho(x)\rho(x-r) dx \quad (2)$$

Figure 3a is a schematic representation of $\rho(r)$ and the corresponding $p(r)$. The $p(r)$ of a lamellar structure with sharp interfaces, fixed thicknesses, and fixed spacing contains an initial linear region followed by a plateau and a sharp first-order peak with a fwhm equal to the

base width, D , of the initial region. According to Babinet's principle,¹⁰ interchange of electron densities of the amorphous and crystalline phases does not affect either the correlation function or the scattering curve. Therefore the base width of the initial region, D , in the correlation function may represent either the amorphous or crystalline lamellar thickness due to this phase identification problem inherent in X-ray scattering. Crystallinity of samples must therefore be obtained by other methods such as differential scanning calorimetry (DSC) to discern whether the SAXS crystallinity ($=D/L$) obtained from the correlation function represents the volume fraction of crystallites or the volume fraction of amorphous domains. Crystallinity considerations¹¹ reveal that the base width, D , of the $p(r)$ function for HDPE represents the amorphous domain thickness of 8 nm. For the case of UHMWPE a variable initial slope, the absence of a plateau region, a skewed nearest-neighbor peak, and crystallinity values close to 50% exacerbate the phase identification problem.

Panels b–d of Figure 3 are plots of selected $\rho(r)$ functions and their corresponding $p(r)$ generated using program DECON developed by Glatter.⁸ Such $\rho(r)$ functions can be used as inputs to program DECON, which performs the autoconvolution to generate corresponding $p(r)$ functions. These figures reveal separately the effects of (b) diffuse interfaces, (c) nonuniformity in the thickness of the amorphous region at constant long period, and (d) changes in the long period. The curvature of $p(r)$ near the origin can be uniquely attributed to the presence of diffuse interfaces in the case of UHMWPE relative to HDPE (Figure 3b). A change in long period does not have an effect on the slope of the initial region (Figure 3d). The variation in the initial slope of the $p(r)$ of UHMWPE can be attributed to the presence of a morphology containing a wide distribution of lamellar (or amorphous zone) thicknesses. A qualitative argument may be made for the presence of a significant population of thick lamellae, which produces a changing slope of the initial region of $p(r)$ as revealed by Figure 3c. This argument is reinforced by skewing of the first-neighbor peak toward larger interlamellar

spacing expected between thicker lamellae (see Figure 3d). Quantitative estimates of the relative fraction of these lamellae would contain errors caused by contributions from diffuse interfaces to the initial linear region. Both the variation in lamellar thickness and interlamellar spacing contribute to the increase in the width of the first-neighbor peak. In the case of UHMWPE this variation is sufficiently large to cause an overlap of the initial linear region and first-neighbor peak in the PDDF.

Conclusions

SAXS analysis by indirect Fourier transformation of the scattering function is a powerful tool in revealing the lamellar morphology of polymers with a low degree of order. Ram-extruded UHMWPE contains a lamellar morphology with large interfacial thickness, a large distribution of lamellar thicknesses, and a large variation in interlamellar spacing as compared to those features in melt-crystallized HDPE. There is a significant number of lamellae with thicknesses and spacing above the average values in the case of UHMWPE.

Taken overall, we conclude that the nanoscale morphology of UHMWPE is clearly different from that of the HDPE, but there remain several possibilities for explanation of their differences. The relatively larger thicknesses, interfacial zones, and nonuniformity in periodicity could be explained by spatially separated "zones" of distinct morphologies in the material or a more uniformly interdigitated construct. We are presently engaged in further experiments to resolve these interesting issues.

Acknowledgment. The authors thank Professor O. Glatter of the Institute of Physical Chemistry, University of Graz, Austria, for providing computer programs ITP and DECON. A.B. acknowledges financial support from the MIT-Brigham and Women's Hospital-Industry Consortium, H.S. the Erwin-Schrödinger Foundation, and R.E.C. the Bayer Professorship in Chemical Engineering at MIT.

References and Notes

- (1) Tsvankin, D. Y. *Polym. Sci. USSR (Engl. Transl.)* **1965**, 6, 2304.
- (2) Vonk, C. G.; Kortleve, G. *Kolloid Z. Z. Polym.* **1968**, 220, 19-24.
- (3) Strobl, G. R. *J. Appl. Crystallogr.* **1973**, 6, 365.
- (4) Strobl, G. R.; Schneider, M. *J. Polym. Sci., Polym. Phys. Ed.* **1980**, 18, 1343.
- (5) Strobl, G. R.; Schneider, M. J.; Voigt-Martin, I. G. *J. Polym. Sci., Polym. Phys. Ed.* **1980**, 18, 1361.
- (6) Glatter, O. *J. Appl. Crystallogr.* **1977**, 10, 415.
- (7) Glatter, O. *Acta Phys. Austriaca* **1977**, 47, 83.
- (8) Glatter, O.; Hainisch, B. *J. Appl. Crystallogr.* **1984**, 17, 435.
- (9) Wagner, H. L.; Dillon, J. G. *J. Appl. Polym. Sci.* **1988**, 36, 567.
- (10) Baltá-Calleja, F. J.; Vonk, C. G. *X-ray Scattering of Synthetic Polymers*; Jenkins, A. D., Ed.; Elsevier New York, 1989; p 282.
- (11) Galeski et al. (*Macromolecules* **1992**, 25, 5705) reported a crystallinity of 64.5% for compression-molded specimens or Petrothene HDPE using DSC. The crystallinity of extruded rods of UHMWPE determined by DSC is $50 \pm 3\%$ (P. Venugopalan and E. W. Merrill, personal communication).

MA950284L